Optical investigations of physiology: a study of intrinsic and extrinsic biomedical contrast*

BRITTON CHANCE[1], QINGMING LUO[1], SHOKO NIOKA[1], DAVID C. ALSOP[2] AND JOHN A. DETRE[3]

[1] *Johnson Research Foundation, Department of Biochemistry and Biophysics, University of Pennsylvania, Philadelphia, PA 19104–6089, USA*
[2] *Department of Radiologic Science, University of Pennsylvania, Philadelpia, PA 19104–4283, USA*
[3] *Department of Neurology, University of Pennsylvania, Philadelphia, PA 19104–4283, USA*

SUMMARY

The utility and performance of optical studies of tissue depends upon the contrast and the changes of contrast in health and disease and in functional activity. The contrast is determined both by the optical properties of extrinsic and intrinsic chromophores and scatterers but especially upon the changes evoked by physiological activity and pathological states. Here, we have focused upon absorption changes of the intrinsic probe, blood absorbance changes due to cortical hypoxia and to haematomas, giving, for particular conditions, absorbance changes of 0.15 and over 0.4 ΔOD, respectively. Functional activity may give changes of blood volume of over 0.05 ΔOD with some variability due to individual responses that is best expressed as histogram displays of the distribution of response among a significant population. Responses have been observed in prefrontal parietal and occipital functions (242 tests). Extrinsic probes afford signals dependent upon the dose tolerance of the subject and can readily equal or exceed the blood volume and oxygenation signals, and currently afford vascular volume and flow indications. However, contrast agents for the functional activity of cellular function are ultimately to be expected. Finally, light-scattering changes afford osmolyte-related responses and are here shown to indicate a large signal attributed to cortical depolarization and K^+ release in hypoxia/ischaemia. Thus, the optical method affords imaging of manifold contrasts that greatly enhance its specificity and sensitivity for diagnostic procedures.

1. INTRODUCTION

I will discuss the kinds of contrasts that will be useful in human studies, a number of examples of their use and some predictions for the future.

Optical contrast is most advantageously obtained using short pulses or amplitude or phase modulation. However, much information can be obtained with the path length scrambled DC signals obtained with continuous light. This has been the classical method for a number of years; it can be implemented with flashlight bulbs, optical filters and silicon detectors in the way that Millikan, my thesis advisor at Cambridge, developed with a split Siemens photovoltaic cell, and a couple of optical filters, a differential amplifier or a summing amplifier. Thus, we will point to the parallels between Millikan's muscle oximeter and the one that we have further developed for measurements in human limbs (Millikan 1937*a*, *b*) (figure 1), and most recently, the component of an imager. First, Millikan employed transmission through the excised cat soleus muscle and was able to use green and orange wavelengths in the visible region with simple colour filters and a split Siemens photovoltaic cell. Its recording was quite sensitive since a fast and responsive galvanometer was used to record the imbalance of the current at the two wavelengths.

The system that we evolved depends upon the classic observations & ingenuity of the yesteryears. Severinghaus & Astrup (1987) have researched the origins of tissue spectroscopy and traced spectroscopy of blood in the human hand to the 1870s (Von Vierordt 1876) and then to Nicholai's (1932) filter wheel apparatus for the finger spectroscopy in normoxia and ischaemia (see also Kramer 1951). In the 1930s Kramer constructed a single-beam apparatus using the Siemens barrier layer detector (Kramer 1935; see also Kramer & Sarre 1935) which he provided for Millikan in 1936, who split the cell to make an effective dual-wavelength haemoglobinometer. At the same time, Matthes & Gross (1939) perfected an ear oximeter which both Kramer and Millikan were soon to adopt in World War II (see Severinghaus & Astrup 1987). Post World War II, the Radiation Laboratory of MIT released its unique electronic technologies and a time-sharing dual-wavelength tissue spectrometer was readily constructed

* Dedicated to the memory of Glenn Millikan who introduced me to tissue spectroscopy in 1937 at the Physiological Library, Cambridge, UK.

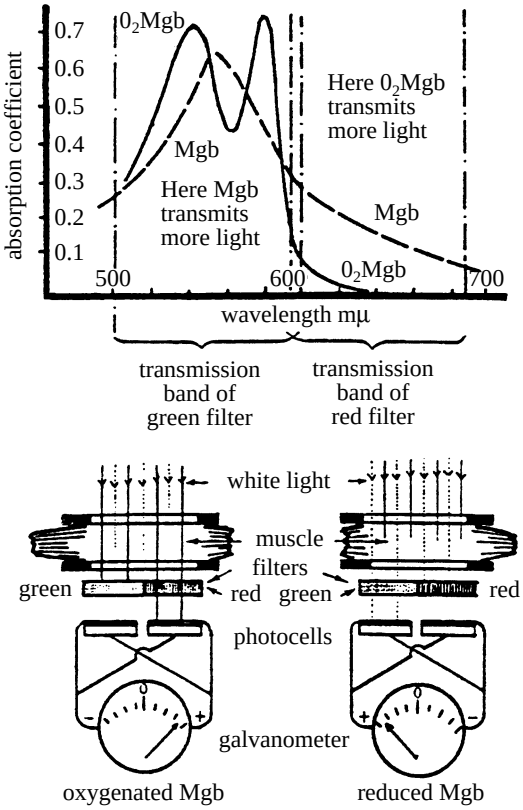

Figure 1. Millikan's dual-wavelength spectrophotometer.

(see also Lubbers & Niesel 1959; Butler & Norris 1960; Smith 1977) which evolved into many filter wheel designs. Jöbsis (1977) evolved a multisource system and has been applying it to the original since 1970. He attempted the much more difficult feat of cytochrome oxidase assay at 830 nm, as had been studied by the London group (Wray *et al*. 1988) especially, and by others as well (Wickramasinghe *et al*. 1986)

For the purpose of tissue spectroscopy, with high contrast and high sensitivity, we have revisited Millikan's dual-wavelength technology with modern technology and have found it to be very efficient for measuring small differences of absorption and rejecting changes of background light scattering since the two wavelengths were quite close together and could be selected by a pair of monochromators (figure 2, Chance 1951). Thus, it was obvious that the dual-wavelength system had the capability to pick up small differences of absorption against a fixed or variable background of light scattering or absorption.

It seemed natural to use this principle for near-infrared (NIR) measurement of the characteristics of haemoglobin absorption in the near-infrared region (see Lemberg & Legge 1949); for example, where wavelengths of 760 nm would be responsive to the deoxy form, the wavelength of 850 nm is responsive to the oxy form, and the difference between the two was very nearly balanced in intensity by using filters of appropriate transmission bandwidth, as has been demonstrated for the dual-wavelength time-shared spectrophotometer (figure 3). Thus, very little electrical offset in the output was necessary to give a null signal for normoxic states, i.e. approximately 60–70 % oxyhaemoglobin, and a large imbalance for changes therefrom in hypoxia and ischaemia (Chance *et al*. 1992).

The transmission of the interference filters was designed so as to achieve approximate imbalance for the normoxic state of tissue, muscle or brain, and highly significant imbalance if the saturation changed. An innovation developed for the study of alcohol dehydrogenase is also employed in which the sum of the absorbances at the pair of wavelengths was used to give the total amount of the pigment involved (Theorell & Chance 1951). In this study we have adopted the same principle and the contributions at the two wavelengths are adjusted so that oxy–deoxy changes are rejected and the sum, i.e. blood volume is accepted. This is accomplished by simple algebraic expression, i.e. 0.1×760 signal plus the total 100 % of the 850 signal. This appears to give reasonable rejection of the oxygenation changes in the middle region of saturation. Obviously, the approximation is saturation dependent but appears to be valid for the normoxic state of brain tissue in which the changes of blood volume are expected to be small for functional activation.

Since the source–detector system RUNMAN is used in the imager described below, we can reproduce its calibration data here as relevant to the performance of the imager. We will also validate its performance in measuring muscle and brain. One can calibrate the response to oxygenation and deoxygenation of haemoglobin in a yeast/blood/intralipid model and demonstrate whether or not the simple arithmetic algorithm rejects, *in the sum channel*, the changes of oxy-

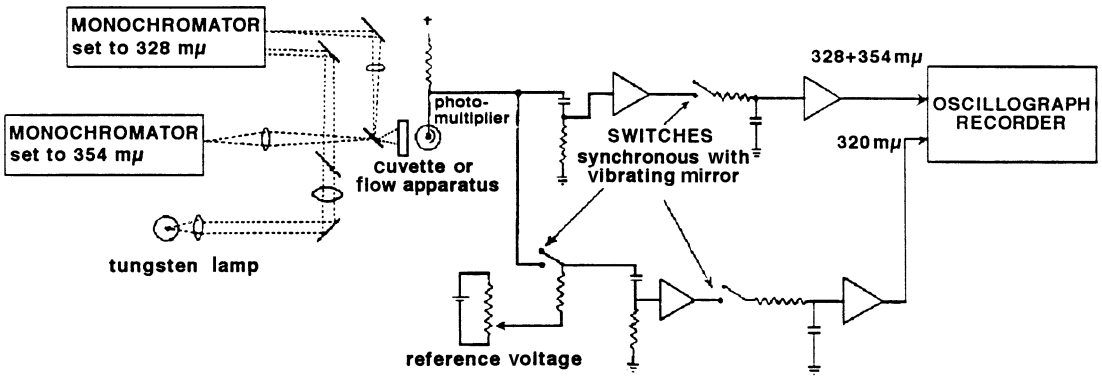

Figure 2. Dual-wavelength time-shared spectrophotometer (Chance 1951).

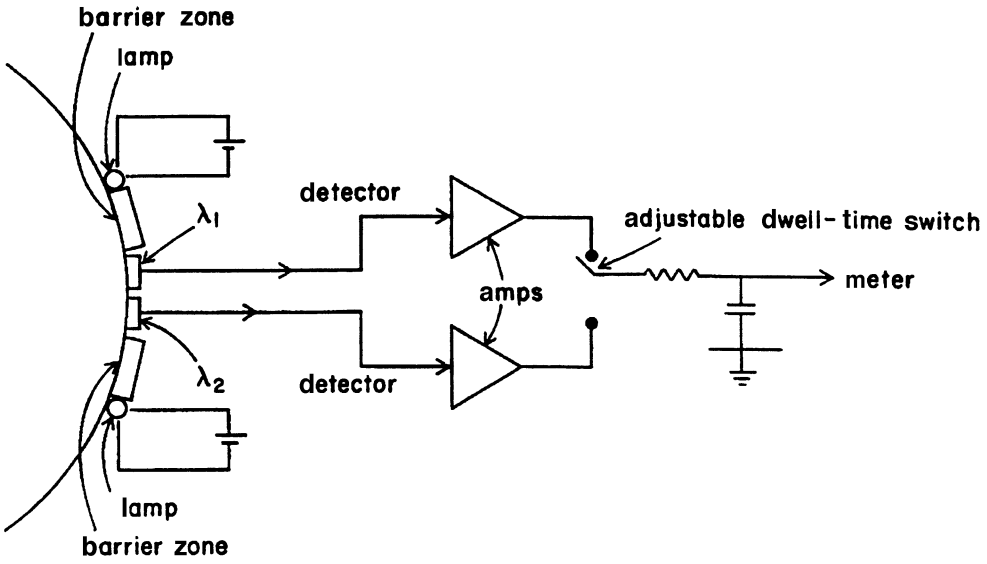

Figure 3. Diagram of RUNMAN principle with difference signals indicated.

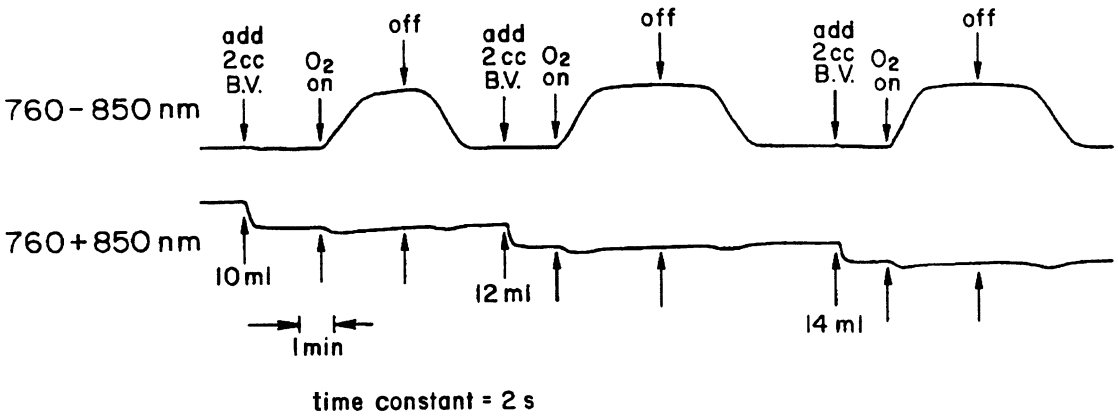

Figure 4. Test of the RUNMAN for blood volume and oxygenation interference.

to deoxyhaemoglobin on the addition of blood (figure 4), and *in the difference channel*, the changes of blood concentration for conditions simulating the brain (μ_a = 0.02, $\mu_s' = 5$–10, and 5–10% blood). There is no detectable cross-talk in the difference channel in the model. In order to evaluate *in vivo* the cross-talk from oxy/deoxy changes in the blood concentration measurement, studies of muscle can be undertaken (Ferrari *et al.* 1995).

There is also a large optical contrast between a muscle in which the arteriovenous circulation has previously been occluded and is released to cause only a venous occlusion (*ca.* 100 Torr) (figure 5). This causes arterial blood to fill the muscle. As shown in figure 5, this increase of blood concentration causes very little cross-talk into the oxy/deoxy channel. Then, when the cuff is completely released, a release of the occluded blood and an infusion of oxygenated blood into the previously deoxygenated muscle is observed, as is the release of accumulated blood. These changes of absorption of blood concentration and oxygenation constitute the foremost contrast of tissues.

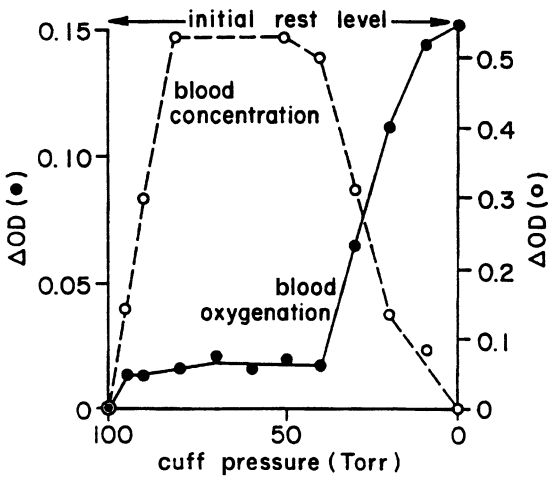

Figure 5. Illustration of the independence of the blood oxygenation recording of the large change of blood volume in muscle with venous occlusion.

(*a*) *Contrast in brain hypoxia: the signal magnitude*

The contrast of highly vascular brain tissue underlying skin and skull is high. The brain is the most actively metabolic organ of the body and has a large

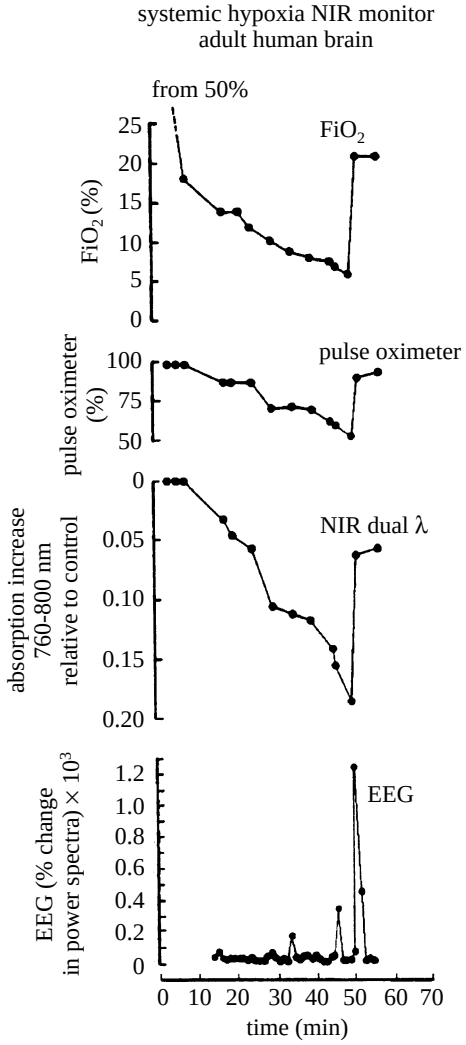

Figure 6. Brain hypoxia study with EEG, pulse oximeter and FiO_2.

blood supply from many vessels appropriate to blood imaging. The contrast has been evaluated by the continuous light device RUNMAN. Such a continuous light probe has a source–detector separation of 4 cm. Dr David S. Smith, a colleague of Dr Warren Levy and ourselves was monitored and was able to undergo hypoxia down to 7 % inspired O_2 (FiO_2) (figure 6). At that point the EEG showed activity bursts indicating functional brain hypoxia. A very large differential absorbance change of about 0.15 ΔOD is measured on the forehead by the dual-wavelength spectrophotometer. This is expected to be at least 50 % of the maximum signal that could be obtained in brain hypoxia.

(*b*) *Contrast in haematomas*

Delpy (1997) presented model data which suggested that the photon diffusion pattern could be confined to just the inner side of the skull. To the contrary, the above studies together with those of Dr Claudia Robertson on cranial haematomas suggest the ready detectability of absorbance changes in the brain (figure 7) (Robertson *et al*. 1994; Gopinath *et al*. 1995). In the case of a cranial bleed in the human brain, this unilateral haematoma is detected by comparing the contralateral side with the ipsilateral side. A ΔOD difference is 0.42. X-ray computed tomography (CT) verifies the intracranial brain bleed. The haematoma consists of shed blood and approaches the 8 mM value for 40 of blood in the arteries and veins, and it accumulates in a much larger volume than in the neighbouring vascular bed (about 4–8 % of the tissue volume). The haematoma was removed surgically, but recurs as a subdural haematoma with a ΔOD of 1.1.

(*c*) *A brain function imager*

The dual-wavelength principle has been adopted for a continuous light imager, where 16 combinations of sources and detectors can be used; nine light sources illuminate the proximal detector pair consecutively for an interval of 0.5 s, thus 8 s are required for a complete cycle of data acquisition (figure 8). The outputs of the optical probe are connected to a 12-bit A-D, set to have a minimum step of 0.304 mV comparable to the noise level of the optical detector/amplifier. The absorbance values during functional activity are computed from DC signals and are subtracted from the values at rest (the data set is normalized for the rest conditions and absorbances are calculated with respect to the rest values). These absorbances are then processed by a direct back projection algorithm and are presented as a 64-pixel image based upon all possible combinations of source/detector from which adequate signals are obtained. The iteration time is 8 s and usually four iterations (32 s) are averaged from the activated state and subtracted from the corresponding values for the resting state. The contouring can be ΔOD = 0.002 but is usually 0.01, appropriate to the absorbance changes and the scale of ± 0.04 and occasionally ± 0.15 (these are $\log_{10}$ values as customary in biochemistry (Lemberg & Legge 1949).

(*d*) *Absorption contrast in brain functional activity*

We term this functional near-infrared imaging (fNIRI). We have focused our studies on brain function since activity minus rest images are readily obtained. Brain function signals afford a contrast due to blood volume and further oxygenation changes. These studies present only the blood concentration changes as represented by the proportioned sum to the two wavelengths. The difference signals representing oxygenation and deoxygenation changes have also been recorded but are beyond the scope of this preliminary report. However, oxygenation of the brain cortex occurred in the majority of the patients but some distinctive deoxygenations were also recorded as were reported in detail elsewhere (Chance *et al*. 1997*a*).

The continuous light imager described above is applied to the sensory-motor region where finger-stroking activity for 10 s gives replicate parietal images (figure 9). The data set of 8 s duration is iterated four times and is subtracted from the rest values (Chance *et al*. 1997*a*). The localized peaks are shown as is the scale of ΔOD $\log_{10}$. We can convert our values to 'micromolar' (Delpy 1997): we calculate the ΔOD of 0.050 corresponding to 4 mM or about 10 % of the changes in the pig brain hypoxia as reported by Matcher *et al*. (1995).

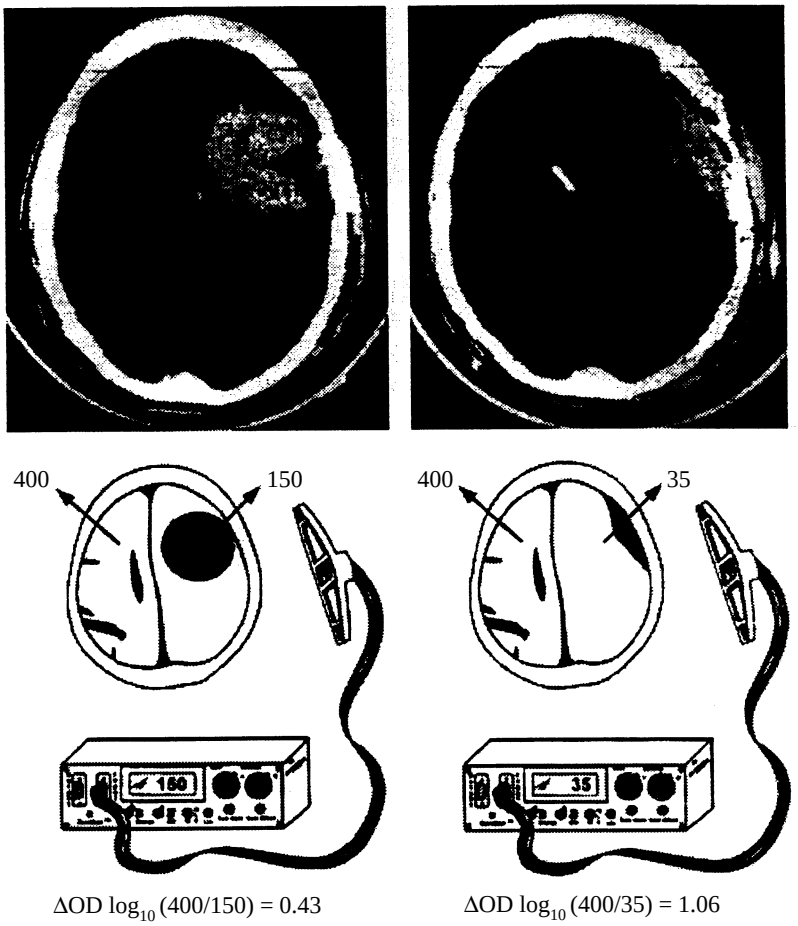

Figure 7. Brain haematoma study: comparison of X-ray, CT and RUNMAN haematoma detection. On the left is an intracranial haematoma ($\Delta OD = 0.43$) and on right is an epidural haematoma ($\Delta OD = 1.06$). Example of a patient who developed both intracerebral and extracerebral haematomas. The top row shows the serial CT scans, and the bottom row shows the NIRS examination at the time of the CT scan. The patient was admitted following an motor–pedestrian accident with a Glasgow Coma Scale of 6 and a CT scan showing a left frontoparietal contusion. The patient was admitted to the hospital and monitored. Eight hours later, the NIRS suggested the development of an intracranial haematoma and a CT scan demonstrated a large left frontal intracerebral haematoma. The patient was taken to surgery and the haematoma evacuated. Postoperatively, the ICP returned to normal values, but then gradually increased over several hours. A CT scan on the second postoperative day showed a postoperative epidural haematoma, which was surgically evacuated (Gopinath 1995).

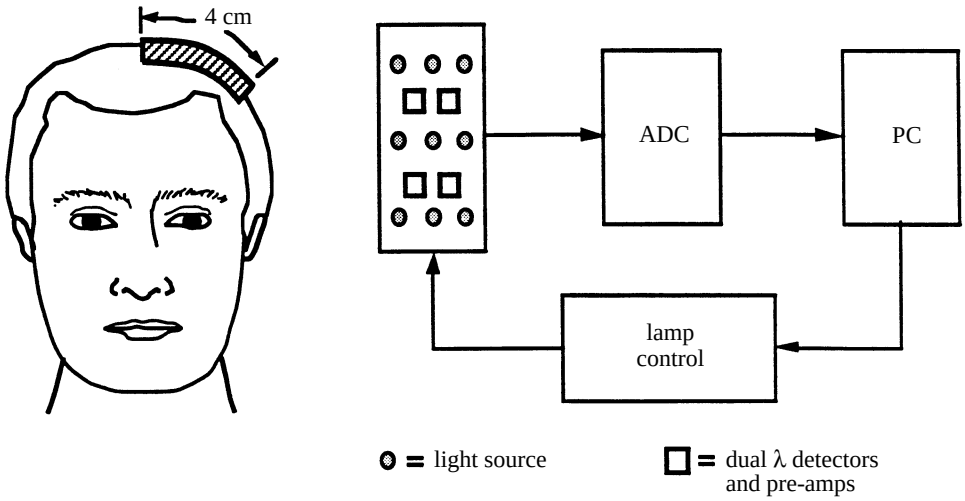

Figure 8. Diagram of the imager (CWI) (continuous wave imager) for parietal region: nine sources, four dual-wavelength RUNMAN detectors.

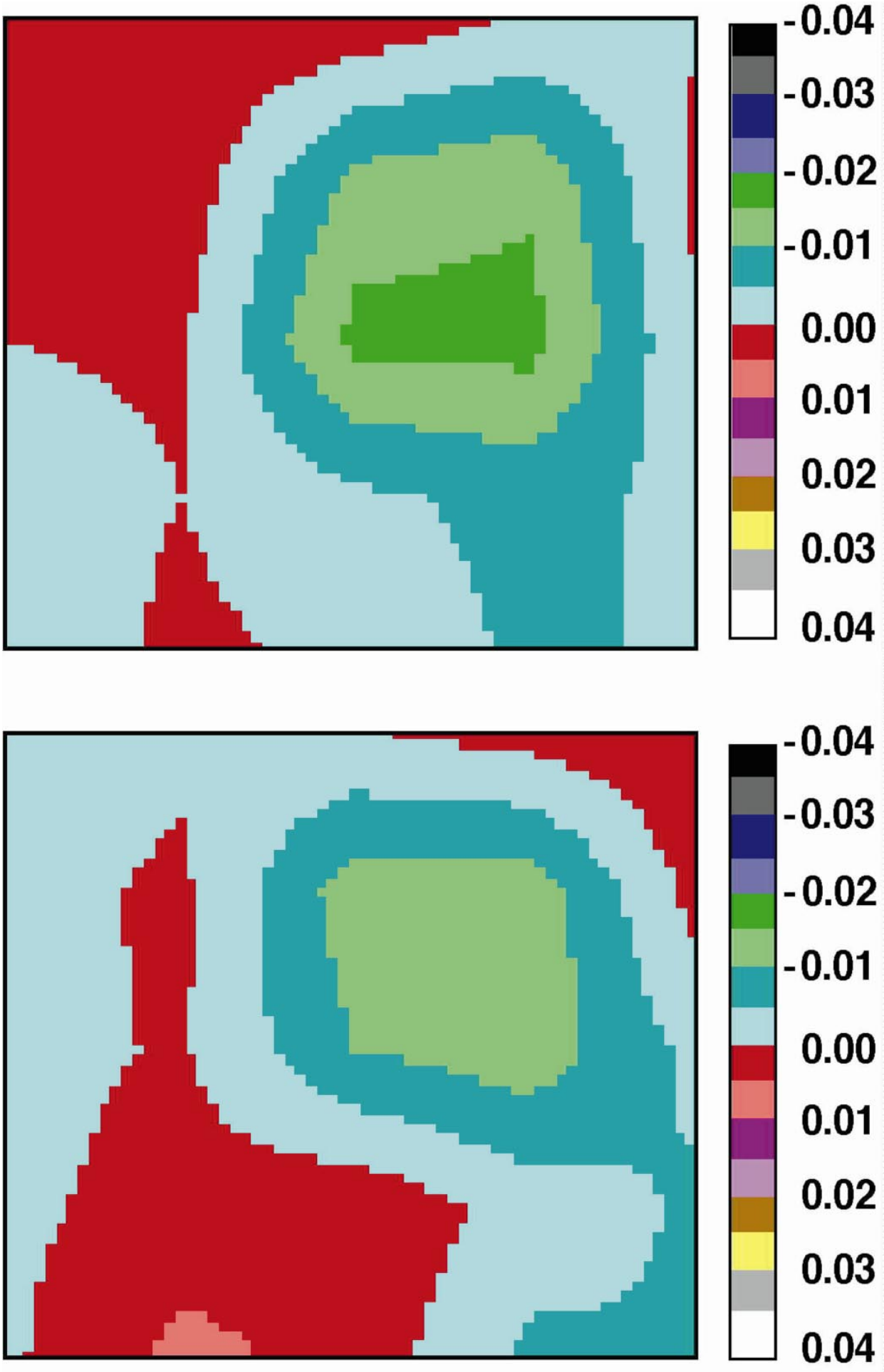

Figure 9. For caption see opposite.

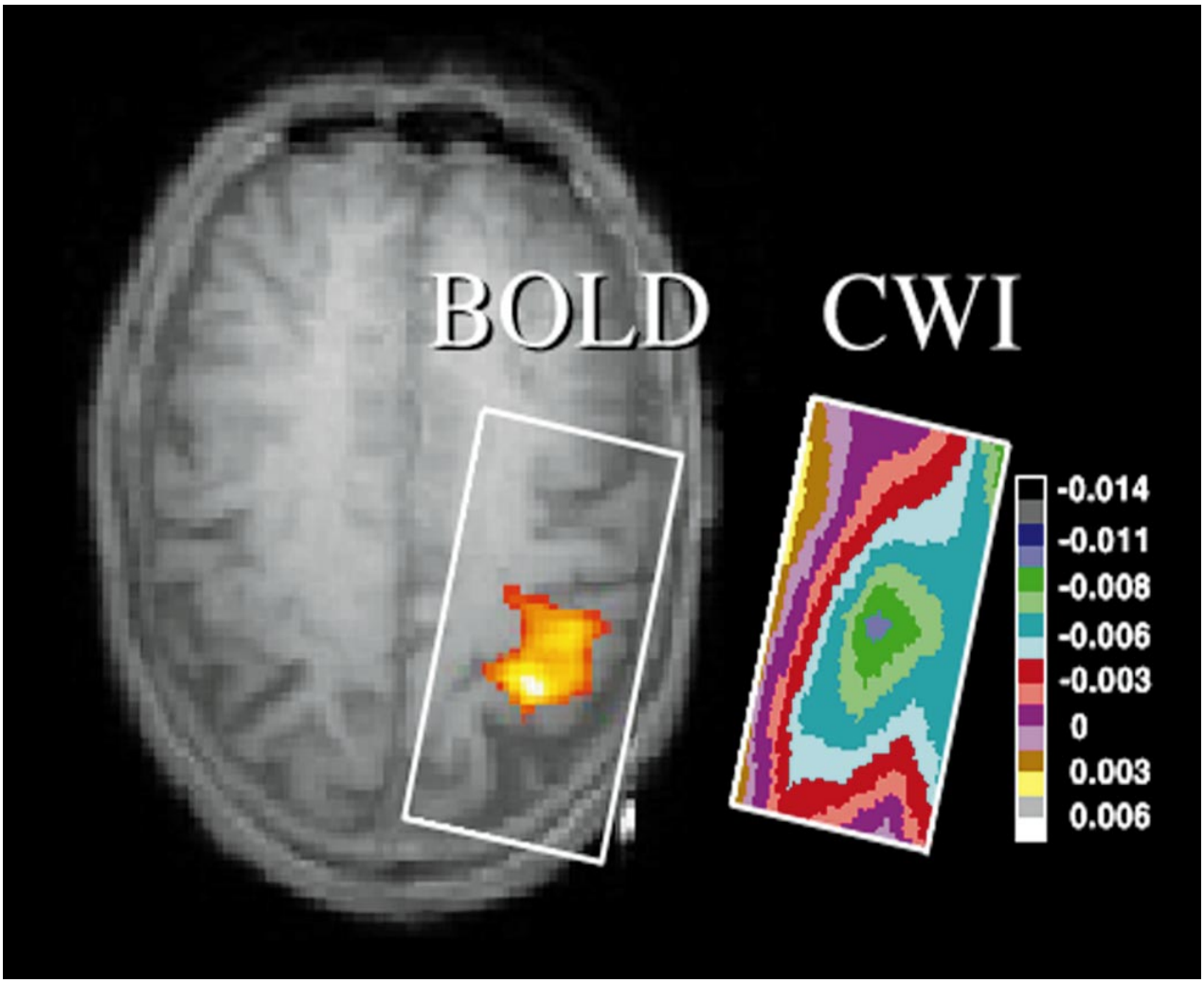

Figure 10. Co-registration of sensorimotor response of BOLD image (left) and CWI (right) and co-registered in the rectangle by water-filled capillaries (1 mM $CuSO_4$) (not shown). BOLD 4.0 T, 30 s stimulation, 30 s rest, 4 min for tactile stimulation. CWI shows the same contours every 0.002 ΔOD; 1 min rest, 1 min tactile stimulation. Both images show blood concentration increases. Courtesy of J. Detre and J. Alsop.

(*e*) *Scaling*

The charts are autoscaled to the largest peak in the image and thus the OD scale is autoscaled and fits the span from the largest to the smallest signal.

(*f*) *Co-registration*

How does this image co-register with functional nuclear magnetic resonance (fNMR)? We placed filled tubes with water and 1 mM copper sulphate at the corners of the optical probe to identify the optical position on the parietal region in the magnetic resonance image (MRI). We then obtained the fMRI of the parietal region activated by stroking fingers with a 4 T MRI. The image required four 30 s on/off intervals. A separate finger-stroking study with the optical imager pad fitted into the copper sulphate defined rectangle was recorded and imaged for a similar interval (figure 10). The fMRI is projected at the surface of the brain and can be compared to the displaced optical image in figure 10. There is rather good congruence of the two images. The shape is not exactly the same and correspondence between the two peaks is accurate to about 2 mm. This is in surprisingly good agreement because fMRI measures larger vessels and deoxyhaemoglobin, and the optical method measures total oxy- plus deoxyhaemoglobin in the capillary bed. This co-registration is important in order that other groups can compare their results and it affords a gold standard for imager performance.

(*g*) *Contrast in a population study*

Variability can be studied in a normal brain population and we have been lucky to have a number of subjects working actively on fNIRI. Sixty-four trials on three bald subjects (figure 11) have been executed. There are 31 significant increases (> 0.02) and 12 decreases of blood volume changes in bins > 0.02.

Figure 9. CWI image of parietal activation: tests of reproducibility of blood volume indication contours are OD according to colour slide. Negative values of OD indicate increase of absorption with respect to rest ($\log_{10} I/I_0$).

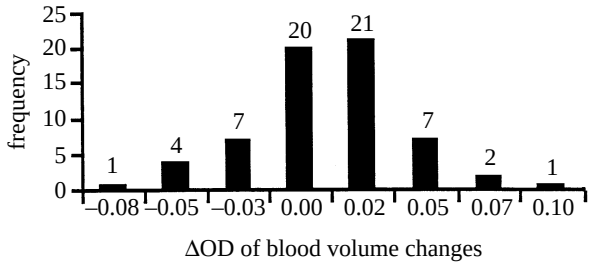

Figure 11. Histogram display of 63 (three subjects) cortical responses of parietal responses to finger tapping, activity minus rest in a region co-registered with 4 T fMRI. The signals are measured at the peak position and represent the ΔOD between tapping and rest. The ΔOD is blood concentration increase. The bin for any column of the histogram is shown by the vertical indicators on each side of the number representing the mean value of the bin.

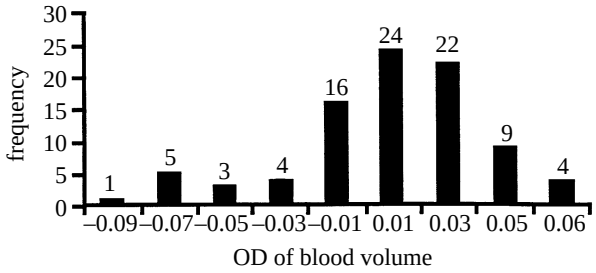

Figure 12. Histogram of blood volume changes due to occipital stimulation with checkerboard pattern.

(*h*) *Occipital region*

Here the contrast is a blood volume change in response to a 7 Hz flashing light. The probe is placed right near the prominent bone on the back of the head and both eyes are stimulated (figure 12). The ΔOD signals are again large and localized to about 1 cm^2 for two repetitions of stimulation. The first stimulation gave a ΔOD of 0.1 and the second a ΔOD of 0.15 in about 1 cm^2 of the surface shown in the highest contour level. Here again, 86 trials with three subjects are shown in the histogram. There is predominantly an increase of blood volume (60 trials) in the region of interest, with 20 decreases. In this case, we have included signals in the 0 to 0.01 bin.

(*i*) *Contrast in the prefrontal region*

Here, cognition signals are obtained with the probe near the midline of the frontal region; the 4 cm width covers the area from the eyebrows up to the hairline. The stimulus is afforded by use of a part of the US Standard Achievement Tests (SAT) and the appropriate analogy between two words is found in the exhibited word list. The test is usually about a minute or two, otherwise we find that attention is lost.

The images show blood volume increases, and the focal point of activity has been observed to move in one case from the peripheral locus to a more central one. The histogram (figure 13) displays 192 studies of 12 subjects and shows that the blood volume increase is the rule (91 trials), but some show a blood volume

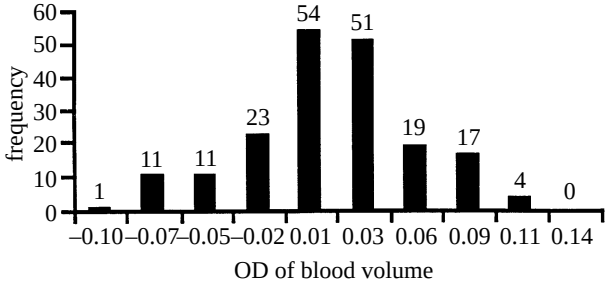

Figure 13. Histogram of blood concentration changes due to prefrontal region stimulation with the SAT test.

decrease (46 trials) attributable to incapability to respond or to factors unknown. In this case, bins > 0.01 are scored.

Obviously, the quality of these images can be vastly improved by using time and frequency-domain methods with spatial Fourier filters (Li *et al*. 1996) but the continuous light method performs adequately for many functional activation studies.

(*j*) *Contrast due to light scattering*

In addition to information on the organelle profile of cells and tissues, the osmotic responses of tissues and organs are sensitively detected, altogether affording sensitive and novel contacts for optical studies of tissue. Of these several signals, those due to osmotic responses of glucose and potassium appear to have the most immediate clinical applicability. This signals are properly evaluated by photon migration technology. The utility of non-invasive optical tissue glucose determination has attracted many technical approaches and some basic studies as well, but the signals are small and appear to vary from subject to subject. Perhaps biochemical and physiological aspects of glucose transport to tissues need to be better understood as well as photon diffusion technology. Potassium and sodium gradients are essential for the generation and propagation of neuronal signals, and high concentration gradients are available in functional tissues. Their discharge has already been observed to be related to a light-scattering change as in the early work of Bryant & Tobias (1952) and Hill & Keynes (1949), together with later work on the *Electrophorus* with Keynes (Aubert *et al*. 1964). Most recently, Salzberg *et al*. (1985) have elegantly shown light-scattering responses in brain slab preparations on stimulation. Thus, it seems possible to study responses due to neuronal activity in human brain directly.

Our interest in brain hypoxia has led us to study hypoxia-induced potassium depolarization in rat brain with rather striking results. Light scattering decreases and optical path length increases are nearly as large as those evoked by haemoglobin deoxygenation. The depolarization signals are temporarily distinguished from the haemoglobin signals; the light-scattering change occurs 30 to 60 s after ischaemia or hypoxia.

Thus a signal of energy deficiency is distinguished from the blood signal, both temporally and by light scattering when using time- and frequency-domain technology to deconvolute light absorption and

scattering. Also, with multiwavelength recordings, the relative independence of scattering upon wavelength distinguishes it from absorption. Thus, the K^+ depolarization seems to afford a unique measure of bioenergetic failure in the brain cortex and thus may have significant clinical application related to the survival of depolarized tissue (Chance *et al*. 1997*b*).

(*k*) *Exogenous contrast agents*

The ultimate contrast is provided by exogenous probes whose optical properties and concentration can be adjusted to afford adequate contrast with respect to the above mentioned intrinsic contrasts and background signals. Furthermore, the exogenous contrast can cause absorption and/or scattering. The available NIR contrast agent is indocyanine green (ICG) with a high extinction coefficient (*ca*. $200\ cm^{-1} \times mM^{-1}$ at 800 nm). This agent gives vascular bed volume (arterioles, capillaries and venules) and it extravasates readily in tumours. Other contrast agents of interest are those under development for photodynamic therapy, porphyrins, phthalocyanine and five-membered porphyrin-like compounds. Adaptation of the contrast agents to the 'NIR window' is in progress in many laboratories and it is expected that membrane potential, Ca^+ levels and antigen–antibody responses may soon be imaged in human tissues.

The experimental data on parietal, occipital and frontal responses were obtained by minority high school and college students in a summer study programme funded by a special fund of the University City Science Center, Philadelphia, USA, and by NASA SHARP PLUS Program. The mentors for this program were David Wright, Perdita Permaul, Tarina Charleston (University of Pennsylvania) and Veresta B. Johnson-Hyman (Edison High School, Philadelphia), together with students from Edison and Girls' High Schools. The data will be reported in detail by this group. The work was also supported in part by NIH grant NS 27346 and the Human Frontiers Science Program (HFSP). Mr Chilton Alter gave invaluable assistance to the studies.

REFERENCES

Aubert, X., Chance, B. & Keynes, R. D. 1964 Optical studies of biochemical events in the electric organ of electrophorus. *Proc. R. Soc. Lond.* B **160**, 211–245.

Bryant, S. H. & Tobias, J. M. 1952 Changes in light scattering accompanying activity in nerves. *J. Cell. comp. Physiol.* **40**, 199–219.

Butler, W. L. & Norris, K. H. 1960 The spectrophotometry of dense light-scattering material. *Arch. Biochem. Biophys.* **87**, 31–40.

Chance, B. 1951 Rapid and sensitive spectrophotometry. III. A double beam apparatus. *Rev. Scient. Instrum.* **22**, 634–638.

Chance, B., Dait, M. T., Chang, C., Hamaoka, T. & Hagerman, F. 1992 Recovery from exercise-induced desaturation in the quadriceps muscles of elite competitive rowers. *Am. J. Physiol.* **262**, C766–C775.

Chance B., Hirth, C., Hyman, C., Luo, Q. & Nioka, S. 1997*a* *f*NIRI functional imaging with near infrared. *Brain 97: XVIIIth International Symposium on Cerebral Blood Flow and Metabolism*, 15–19 June, Baltimore. (Submitted.)

Chance, B., Mayevsky, A., Guan, B. & Zhang, Y. 1997*b* Hypoxia triggers a light scattering event in rat brain. In *Oxygen transport to tissue XIX* (ed. D. Harrison & D. Delpy). New York: Plenum Press. (Submitted.)

Ferrari, M., De Blasi, R. A., Fantini, S., Franceschini, M. A., Barbieri, B., Quaresima, V. & Gratton, E. 1995 Cerebral and muscle oxygen saturation measurement by a frequency-domain near-infrared spectroscopic technique. In *Optical tomography, photon migration, and spectroscopy of tissue and model media: theory, human studies, and instrumentation* (ed. B. Chance & R. R. Alfano). *Proc. SPIE* **2388**, 868–874.

Gopinath, S. P., Robertson, C. S., Contant, C. F., Narayan, R. K., Grossman, R. G. & Chance, B. 1995 Early detection of delayed traumatic intracranial hematomas using near infrared spectroscopy. *J. Neurosurgery* **83**, 438–444.

Hill, D. K. & Keynes, R. D. 1949 Opacity changes in stimulated nerve. *J. Physiol.* **108**, 278–281; *Am. J. Physiol.* **165**, 229–246.

Jobsis, F. F. 1977 Non-invasive, infra-red monitoring of cerebral and myocardial oxygen sufficiency and circulatory parameters. *Science* **198**, 1264–1267.

Kramer, K. 1935 Verfahren zur fortlaufenden messung des sauerstoffgehaltes im stromenden blute an uneroffneten gefassen. *Z. Biol.* **96**, 61–75.

Kramer, K. & Sarre, H. 1935 *Z. Biol.* **36**, 76–110.

Kramer, K., Elam, J. O., Saxton, G. A. & Elam Jr, W. N. 1951 Influence of oxygen saturation, erythrocyte concentration and optical depth upon the red and near-infrared light transmittance of whole blood. *Am. J. Physiol.* **165**, 229–246.

Lemberg, R. & Legge, J. W. 1949 *Hematin compounds and bile pigments*. New York: Interscience.

Li, X. D., Durduran, T., Chance, B. & Yodh, A. 1996 Spectrum approach to biomedical imaging with diffuse photon density waves. *Appl. Opt.* **35**, 3746–3758.

Lubbers, D. W. & Niesel, W. 1959 Der kurzzeit-spektralanalysator, ein schnell arbeitendes, spektral-photometer zur laufenden messung von absorptions-bzw. Extinktionsspektren. *Pflügers Arch. Ges. Physiol.* **268**, 286–295.

Matcher, S. J., Elwell, C. E., Cooper, C. E., Cope, M. & Delpy, D. T. 1995 Performance comparison of several published tissue near-infrared spectroscopy algorithms. *Anal. Biochem.* **227**, 54–68.

Matthes, K. & Gross, F. 1939 Zur methode der fortlaufendent registrierung der farbe des menschlichen blutes. *Arch. F. Exper. Path. U. Pharmakol.* **191**, 523–528.

Millikan, G. A. 1937*a* Experiments on muscle haemoglobin *in vivo*; the instantaneous measurement of muscle metabolism. *Proc. R. Soc. Lond.* B **129**, 218–241.

Millikan, G. A. 1937*b* Experiments on muscle haemoglobin, *Proc. R. Soc. Lond.* B **123**, 218–244.

Nicolai, L. 1932 Über sichbarmachung, verlauf und chemische kinetik der oxyhemoglobinreduktion im lebenden gewebe, besonders in der menschlichen haut. *Pflügers Arch. Ges. Physiol.* **229,** 371–389.

Robertson, C. S., Gopinath, S. P. & Chance, B. 1995 A new application for near-infrared spectroscopy: detection of delayed intracranial hematomas after head injury. *J. Neurotrauma* (Suppl.) **12**, 591–600.

Salzberg, B. M., Okaid, A. L. & Gainer, H. 1985 Large rapid changes in light scattering accompanying secretion by nerve terminals in the mammalian neurohypophysis. *J. Gen. Physiol.* **86**, 395–411.

Severinghaus, J. W. & Astrup, P. B. 1987 *History of blood gas analysis*. Boston, MA: Little, Brown & Co.

Smith, K. C. (ed.) 1977 *The science of photobiology*, p. 400. New York: Plenum Press.

Theorell, H. & Chance, B. 1951 Studies on liver alcohol

dehydrogenase. II. The kinetics of the compound of horse liver alcohol dehydrogenase and reduced diphosphopyridine nucleotide. *Acta. Chem. Scand.* **5**, 1127–1144.

Von Vierordt, K. 1876 *Die quantitative spektralanalyse in ihrer anwendung auf physiologie, chemie und technologie*. Tubingen: H. Laupp'sche Buchhandlung.

Wickramasinghe, Y. A. B. D., Crowe, J. A. & Rolfe, P. 1986 Laser source and detector with signal processor for a near infrared medical application. In *Progress reports on electronics in medicine and biology* (ed. K. Copeland), pp. 209–215. London: IERE Press.

Wray, S., Cope, M., Delpy, D. T., Wyatt, J. S. & Reynolds, E. O. R. 1988 Chracterisation of the near infrared absorption spectra of cytochrome *aa*3 and haemoglobin for the non invasive monitoring of cerebral oxygenation. *Biochim. Biophys. Acta* **933**, 184–192.